

# STUDIES OF PREMIXED LAMINAR AND TURBULENT FLAMES AT MICROGRAVITY

(NASA Grant No. NAG3-2124)

M. Abid, K. Aung, C. Kaiser, J.-B. Liu, P. D. Ronney, J. Sharif  
Department of Aerospace and Mechanical Engineering  
University of Southern California, Los Angeles, CA 90089-1453

## INTRODUCTION

Several topics relating to premixed flame behavior at reduced gravity have been studied. These topics include: (1) flame balls; (2) flame structure and stability at low Lewis number; (3) experimental simulation of buoyancy effects in premixed flames using aqueous autocatalytic reactions; and (4) premixed flame propagation in Hele-Shaw cells.

## STRUCTURE OF FLAME BALLS AT LOW LEWIS-NUMBER (SOFBALL)

The SOFBALL space flight experiments on STS-83 and STS-94 in 1997 showed that spherical, stable, stationary flame structures ("flame balls") could be observed in long-duration microgravity experiments in low Lewis number premixed gases near extinction limits. The resulting data provided the opportunity to study the interactions of the two most important processes necessary for combustion (chemical reaction and heat and mass transport) in the simplest possible configuration.

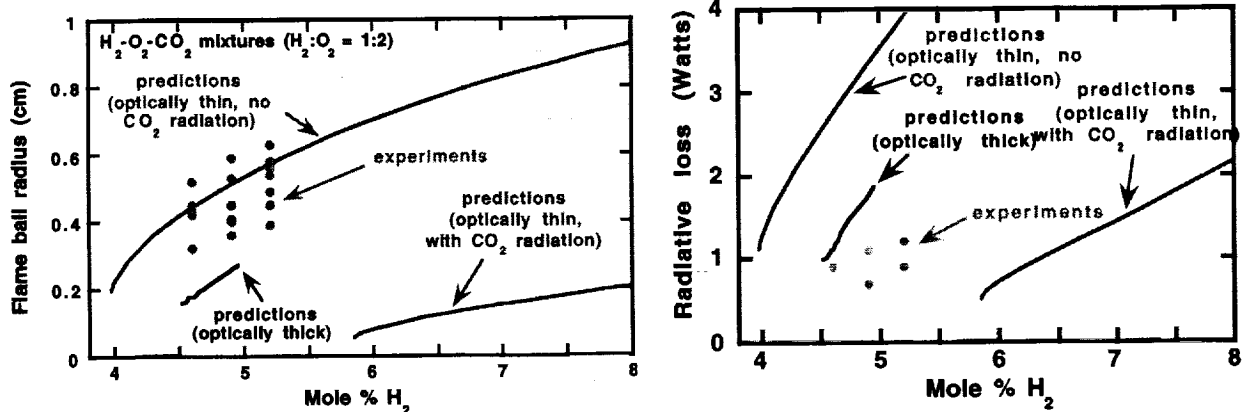


Figure 1. Predicted and measured flame ball properties as a function of fuel concentration for  $H_2 - O_2 - CO_2$  mixtures at 1 atm. Left: radii. Right: radiant power.

Despite their simplicity, flame balls presents a number of interesting challenges to the computationalist. In particular, prior computations comparing results obtained assuming optically thin vs. optically opaque (no transmission)  $CO_2$  radiation suggest that reabsorption of emitted radiation is probably a dominant effect in flame ball mixtures diluted with  $CO_2$ . Consequently, an investigation of the effects of reabsorption of emitted radiation on flame balls was conducted using a numerical code with detailed chemical, transport, and radiative emission-absorption models. A Statistical Narrow Band—Discrete Ordinates method was used to model radiative transport. It was found that reabsorption effects were moderate in  $H_2$ -air mixtures but dominant in  $H_2$ - $O_2$ - $CO_2$  mixtures, due to the fact that in the former case the ambient mixture contains only radiatively inert gases whereas in the latter case  $CO_2$ , a strong absorber, is present in the unburned gas. It was found that reabsorption of emitted radiation led to substantially larger flame ball sizes and wider extinction limits than calculations using optically-thin radiation models (Fig. 1). It was found that for  $H_2$ - $O_2$ - $CO_2$  mixtures, the agreement between model predictions and experimental results was much closer when reabsorption effects were incorporated (Fig. 1). It is concluded that fundamental flammability limits of flame balls can exist

due to radiative heat loss, but these limits are strongly dependent on the emission-absorption spectra of the reactant and product gases and their temperature dependence, and cannot be predicted using gray-gas or optically-thin model parameters.

### FLAME STRUCTURE AND STABILITY AT LOW LEWIS NUMBER

Recent theoretical work on premixed flames by Linan and by Buckmaster and nonpremixed flames by Dold indicate that at low Lewis number, a transition in the structure of stretched premixed flames in a counterflow from smooth or moderately cellular flames to flame tubes may occur near extinction, which enables the flame to survive in the presence of strain that would cause it to extinguish were it forced to remain planar and continuous. This behavior is somewhat analogous to spherically-symmetric flame balls observed in microgravity experiments where in that case radiative transfer rather than extensional strain is the prevailing loss mechanism, but in both cases the Lewis number enhancement of flame temperature causes the curved flame to survive where a plane flame could not. With this motivation, flames in strained  $H_2-O_2-N_2$  mixtures were studied using a counterflow slot-jet apparatus (Fig. 2). Three configurations were examined: single premixed, twin premixed and nonpremixed flames. For all three configurations a wide variety of nonplanar flame structures were observed. Two extinction limits, one at very high strain (corresponding to a residence time limitation) and one at low strain (corresponding to a heat loss extinction) were found (Fig. 3). It was found that as the fuel concentration was decreased for a fixed value of strain rate, the following sequence of behavior was observed (Figs. 3 and 4) —(1) twin wrinkled flames, (2) twin flames with some portions of the two flames merged, a structure which we have termed bridged tubes, (3) isolated tubes which are inevitably travelling in the direction parallel to the stagnation plane, (4) two isolated, stationary tubes, (5) one isolated, stationary tube and (6) complete flame quenching. Both strain-induced and heat-loss induced quenching was observed. At high flow velocities transition to turbulent flow was noted. For nonpremixed flames (not shown), nonplanar flame structures were observed only for near-extinction conditions, but the resulting flame shapes were quite similar to those of premixed flames.

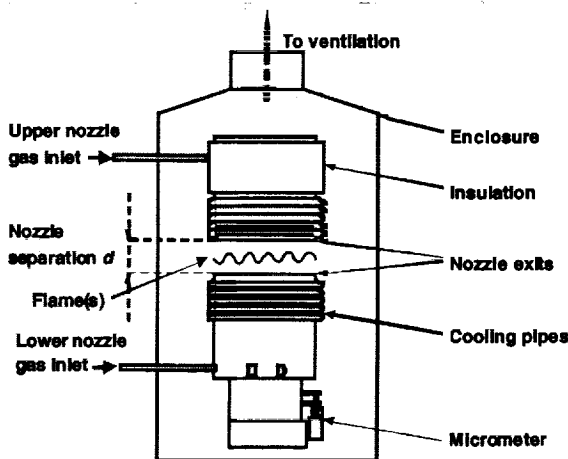


Figure 2. Schematic diagram of counterflow slot-jet burner.

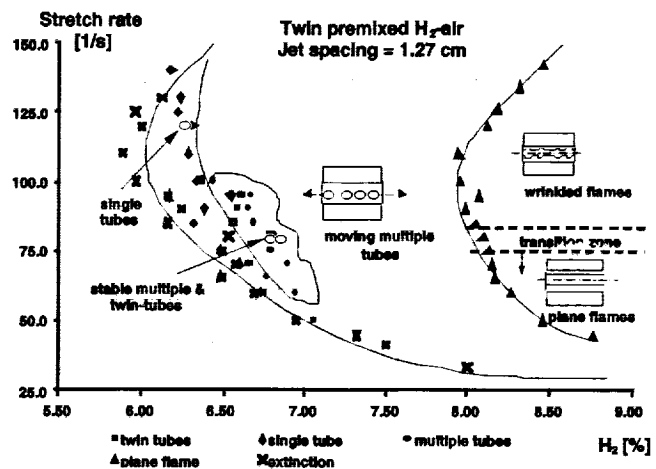


Figure 3. Stability and extinction limits for twin  $H_2$ -air premixed flames.



Figure 4. Shadowgraph images of twin premixed flames. Except where noted, jet spacing is 1.27 cm. (a). Plane flames, 8.26% H<sub>2</sub>, strain rate 60 s<sup>-1</sup>.



Figure 4.(b) Wrinkled flames, H<sub>2</sub> =8.10%, stretch rate 110 s<sup>-1</sup>.



Figure 4.(c) Moving tubes front view, 6.96% H<sub>2</sub>, strain rate 60 s<sup>-1</sup>.



Figure 4. (d) Moving tubes side view, jet spacing 1.35 cm, 6.96% H<sub>2</sub>, strain rate 56 s<sup>-1</sup>.



Figure 4.(e) Twin tubes, 6.68% H<sub>2</sub>, strain rate 60 s<sup>-1</sup>.



Figure 4. (f) Single tube in center, 6.64% H<sub>2</sub>, strain rate 60 s<sup>-1</sup>.



Figure 4. (g) Single tube near wall,, 6.11% H<sub>2</sub>, strain rate 100 s<sup>-1</sup>.



Figure 4. (h). Turbulent flame structure, 6.9% H<sub>2</sub>, strain rate 158 s<sup>-1</sup>.

## LIQUID FLAMES

The PI has introduced the use of aqueous autocatalytic chemical reaction fronts for the experimental simulation of combustion processes. These fronts exhibit little density change across the front, have simple chemistry, are unaffected by heat losses and have high Schmidt numbers, allowing the front to remain flamelet-like even in the presence of very strong flow disturbances or turbulence. Thus, such fronts are useful for experimental study of combustion under conditions more readily simulated by available theoretical and numerical models. Hele-Shaw cells are frequently employed to study buoyancy effects in fluid systems in a simple quasi-two-dimensional geometry where the flow is governed by a linear equation (Darcy's law). Thus, autocatalytic reactions in Hele-Shaw cells represent the simplest possible experimental realization of the interaction of a propagating front with buoyancy-induced convection. We have conducted experiments buoyantly unstable upward-propagating autocatalytic reaction-diffusion fronts and non-reacting displacement fronts in Hele-Shaw cells and found a fingering-type instability (Fig. 5) whose wavelengths ( $\lambda^*$ ) are consistent with an interfacial tension ( $\Sigma$ ) at the front caused by the change in chemical composition, despite the fact that in both cases the solutions are miscible in all proportions. Using the Saffman-Taylor model for the maximum wavelength of disturbances at an interface in a Hele-Shaw cell, the relation  $\Sigma \cong K/\tau$ , where  $\tau$  is the interface thickness and  $K \cong 4 - 2 \times 10^{-6}$  dyne for weak ionic solutions, is shown to enable prediction of the observed values of  $\lambda^*$  for both types of fronts as well as results of several prior experiments on miscible fronts. This value of  $K$  typically yields tensions on the order of 0.005

dyne/cm, which is more than 10,000 times smaller than that of a water-air interface at room temperature, yet this tension has a dominant effect on the observed flow and fingering patterns.



Figure 5. Contrast-enhanced images of interfaces in Hele-Shaw cells. Left: upward propagating reaction-diffusion front with  $s = 0.0038$  cm/s,  $w = 1.0$  mm,  $\delta = 0.00032$ ,  $Pe = 63$ , field of view 5.0 cm wide. Right: non-reacting displacement front of water over water/ethanol solution with  $KMnO_4$  dye,  $w = 0.80$  mm,  $\delta = -0.00036$ ,  $\theta = 180^\circ$ ,  $Pe = 85$ , field of view 5.4 cm wide.

### PREMIXED-GAS FLAME PROPAGATION IN HELE-SHAW CELLS

Premixed gas flame fronts are subject to a number of instability mechanisms that affect their propagation rates and shapes via wrinkling. To obtain a more detailed understanding of these instabilities in a simple geometry, experiments were performed in a 600 mm x 400 mm x 13 mm Hele-Shaw cell using methane and propane as fuel and  $N_2$  or  $CO_2$  as diluents. Upward, downward and horizontal propagation configurations were tested. In this way the effects of buoyancy, thermal expansion and Lewis number were studied. Fronts with a variety of burning velocities ( $S_L$ ) and Lewis numbers were examined. Wrinkling was observed for all flames examined. The burning rates of these flames are quite different from their laminar, unwrinkled values. Values of  $S_T/S_L$  in the quasi-steady stage were higher for upward vs. downward propagation, but only weakly dependent on Lewis and Peclet numbers (Figure 6). These results show that even for mixtures with high Lewis number (stable to diffusive-thermal effects) at microgravity, thermal expansion and viscosity changes across the front will lead to flame instabilities. These results also indicate that the behavior of flame propagation in narrow channels such as crevice volumes in premixed-charge internal combustion engines may be quite different from that inferred from simple laminar flame experiments. This behavior is noteworthy because flame quenching in crevice volumes is an important source of unburned hydrocarbon emissions in these engines.

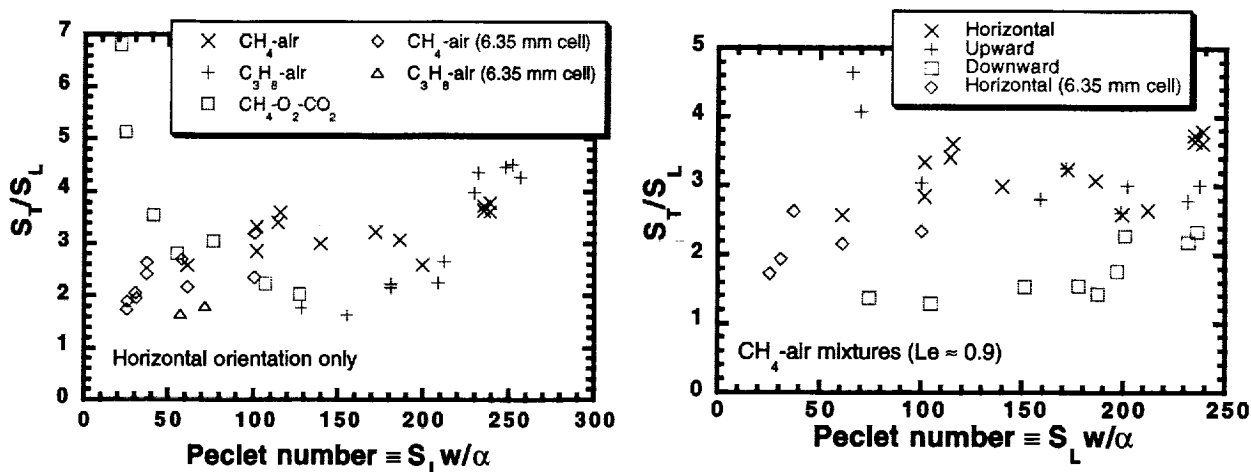


Figure 6. Effect of Peclet number on steady flame propagation speeds (relative to laminar burning velocity). Left: Varying fuel- $O_2$ -diluent combinations having varying Lewis numbers. Right: Varying propagation direction relative to gravity.